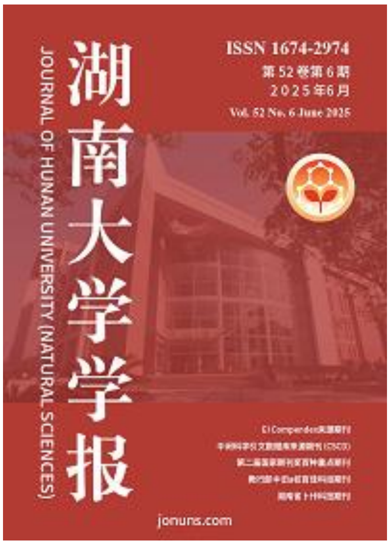

Journal of Hunan University (Natural Sciences)

Vol. 52 No. 6
June 2025

Available online at
https://jonuns.com

Open Access Article

https://doi.org/10.55463/issn.1674-2974.52.6.16

Numerical Evaluation of Cross Necklace and Startail Reinforcement Configurations in MSE Retaining Walls

Karminto [1]*, Roesdiman Soegiarso [2], Indra Noer Hamdhan [3]

[1,2] Engineering Doctoral Program, Universitas Tarumanagara, DKI Jakarta, Indonesia,

[3] Department of Civil Engineering, Institut Teknologi Nasional, Bandung, West Java, Indonesia

* Corresponding author: karminto_008@yahoo.co.id

Article History:
Received: May 23, 2025
Revised: June 28, 2025
Accepted: July 9, 2025
Published: July 31, 2025

Abstract: This study evaluates reinforcement configurations for mechanically stabilized earth (MSE) retaining walls using numerical modelling. The “Cross Necklace” and “Startail” systems are compared against anchor-only baselines across varying center-to-center (CTC) spacings, with horizontal displacement and factor of safety (FoS) used as performance metrics. The configuration featuring a 30 × 30 cm Cross Necklace at a CTC spacing of 30 cm yielded the smallest horizontal displacement (30.5 mm) and the highest FoS (1.67), indicating the greatest stability among the tested models. Increasing CTC spacing systematically increased horizontal displacement. Models without a Cross Necklace or with anchors only exhibited significantly larger deformations; the anchor-only case resulted in 105 mm of displacement and an FoS of 1.44, falling below target stability criteria. Startail configurations showed greater deformation than the Cross Necklace but remained within acceptable safety limits. The superior performance of the 30 × 30 cm Cross Necklace is attributed to its larger cross-sectional area, which enhances interlock with the backfill, increases bearing capacity, and restrains lateral movement. Overall, Cross Necklace reinforcement at reduced CTC spacings offers an effective design solution for minimizing deformation and enhancing stability in MSE retaining walls.

Keywords: mechanically stabilized earth (MSE) wall; Anchors; Cross Necklace; Startail.

MSE 挡土墙中十字项链和星尾钢筋配置的数值评估

摘要：本研究使用数值模型评估了机械稳定土 (MSE) 挡土墙的加固配置。将 “十字项链” 和 “星尾” 系统与不同中心距 (CTC) 的仅锚固基线进行比较，并使用水平位移和安全系数 (FoS) 作为性能指标。30 × 30 厘米十字项链的配置，CTC 间距为 30 厘米，产生的水平位移最小（30.5 毫米）且 FoS 最高（1.67），表明其在测试模型中稳定性最高。增加 CTC 间距会系统地增加水平位移。没有十字项链或仅带有锚固的模型表现出明显更大的变形；仅锚固的情况导致 105 毫米的位移和 1.44 的 FoS，低于目标稳定性标准。星尾配置显示出比十字项链更大的变形，但仍在可接受的安全限度内。 30 × 30 厘米十字项链的卓越性能归功于其更大的横截面积， 这增强了与回填土的互锁， 提高了承载力，并抑制了横向移动。总而言之，减小CTC间距的十字项链加固为MSE挡土墙提供了一种有效的设计方案，可最大限度地减少变形并增强其稳定性。

关键词：机械稳定土（MSE）墙；锚；十字项链；星尾

---

1. Introduction

Retaining structures are designed to stabilize natural or engineered slopes and prevent deformations and failures that could compromise adjacent infrastructure. For mechanically stabilized earth (MSE) walls, performance is influenced by slope geometry, backfill properties, surcharge and seismic loads, and hydraulic conditions behind the wall. Current design guidance emphasizes the need to address both strength and serviceability, with explicit checks for earth pressures, surcharges (uniform and line loads), groundwater and pore-water pressures, and seismic effects [1, 2]. In practice, inadequate drainage and prolonged saturation of the backfill are among the most common precursors to wall distress, as rising water levels increase lateral earth pressure and reduce available shear strength [1-3].

A substantial body of forensic and field evidence links poor hydraulic control to deformations and failures in mechanically stabilized earth (MSE) walls. Koerner and Koerner compiled databases of 171 and later 320 failures of geosynthetic-reinforced MSE walls, many of which involved hydraulic issues—such as low-permeability backfills, clogged drains, or unaccounted hydrostatic pressures, rather than purely structural design errors [3, 4]. Design guidelines and practice papers further emphasize that drainage is not optional: assumptions of “free draining” conditions must be validated, and internal and external drainage systems must be designed for credible storm durations and intensities, as well as monitored and maintained throughout the service life of the wall [1, 5]. These concerns are echoed in European practice: Eurocode 7 stipulates that, in the absence of reliable drainage, the design water level should coincide with the retained ground surface; a lower water level may be assumed only if reliable drainage is provided, and even then, adequate maintenance provisions are required [2].

Beyond drainage, reinforcement layout and spacing significantly influence wall kinematics under wetting conditions. Recent model and centrifuge studies demonstrate that rainfall infiltration and elevated pore-water pressures can increase facing displacement and reinforcement tension, while internal drainage or hybrid reinforcement systems can mitigate these effects [6-8]. However, comparative evidence on alternative reinforcement geometries designed to enhance soil-reinforcement interlock and resist lateral movement under adverse hydraulic conditions remains limited.

This study addresses this gap by introducing and evaluating two reinforcement configurations – Cross Necklace and Startail (“Fish Fins”) – and comparing them with an anchor-only baseline in mechanically stabilized earth (MSE) retaining walls. Using numerical modelling, we quantify the influence of reinforcement geometry and center-to-center (CTC) spacing on horizontal displacement and factor of safety (FoS) under representative hydraulic loading. Specifically, we benchmark the Cross Necklace and Startail configurations against the anchor-only design, examine their sensitivity to CTC spacing, and identify configurations that minimize displacement while meeting target FoS values. Our results indicate that a 30 × 30 cm Cross Necklace at a CTC spacing of 30 cm yields the smallest displacement and highest FoS among all tested configurations. We discuss the implications for reinforcement detailing and drainage provisions in MSE wall design. Hydrostatic pressure, particularly under intense and prolonged rainfall, is a major contributor to MSE wall failures (Figure 1).

(a) MSE Wall collapsed due to hydrostatic pressure

(b) Retaining wall collapse in Kelowna British Columbia, built in 2009, movement occurred on Nov 28, 2011

(c) Toe Failure MSE Wall due to *hydrostatic* pressure and long duration of rain

(d) Built in 2016, movement occurred after being measured with an inclinometer 2021 location Fort Mill Township York County South Carolina, USA

(e) Landslide on Sunday, July 7, 2024 Bintaro Toll Location.

Figure 1. MSE walls failure due to hydrostatic pressure and rainfall (authors' photos)

According to [5], out of 301 MSE wall failures, 191 were attributed to hydrostatic pressure and adverse soil conditions.

This study aims to numerically model the Cross Necklace and Startail ("Fish Fin") reinforcement systems in MSE walls to evaluate their contribution to structural stability. Additionally, the study analyses the effects of variations in anchor length, strip plates, and Startail geometry on wall stability. Furthermore, it investigates how the spacing between Cross Necklace elements along the anchor influences the overall performance and stability of the MSE wall, thereby providing deeper insights into the design and optimization of this soil-retaining system.

2. Materials and Methods

We combined field instrumentation with numerical analysis based on site-specific geotechnical data. Field monitoring included inclinometers to track lateral ground and wall movements, piezometers to measure pore-water pressures in the retained zone, and periodic total station surveys of wall facing targets. Instrument selection and deployment followed established geotechnical instrumentation guidelines for transportation projects [9], with drainage and hydraulic conditions monitored to capture system responses during wet periods.

Numerical simulations were conducted using a finite-element geotechnical software program to evaluate MSE wall performance under both measured and design load cases, including self-weight, surcharges, hydrostatic water pressures, and seismic scenarios where applicable. Model construction, boundary conditions, and soil–structure interaction were defined in accordance with current practice for MSE walls. Program setup and reference documentation were provided by the software developer [10]. Design checks were performed in compliance with SNI 8460:2017 geotechnical requirements and widely accepted practice guidelines for MSE walls, covering both strength and serviceability limit states, such as sliding, overturning, bearing capacity, internal stability, and deformation control [11].

An MSE wall solution was selected due to right-of-way (ROW) constraints, accelerated construction using modular or precast components, and cost competitiveness relative to conventional cast-in-place retaining walls [12].

Serviceability criteria were established to limit horizontal displacement and settlement in accordance with SNI 8460:2017 project classification requirements [13]. To characterize soil–reinforcement interaction for the reinforcement layouts under investigation, a pullout testing program based on ASTM D6706 was planned. Testing was conducted at Jl. Geger Kalong Hilir (Bandung); an earlier plan to carry out tests at Jababeka Industrial Estate (Jababeka IX) was not implemented due to permitting constraints. Laboratory pullout data were used to parameterize interface resistance in the numerical model and to corroborate internal stability checks [14, 15].

According to SNI 1744:2012, page 22, the compaction requirements for the landfill material, specifically red soil, specify a minimum California Bearing Ratio (CBR) of 6.5%, a maximum dry density of 1.5 g/cm³, a design dry density of 1.43 g/cm³, and a minimum compaction degree of 95% of the maximum dry density (Figure 2).

2.1. How Anchor, Cross Necklace, and Startail Reinforcements Work

The structural mechanism of the Anchor, Cross Necklace, and Startail ("Fish Fin") systems is as follows:

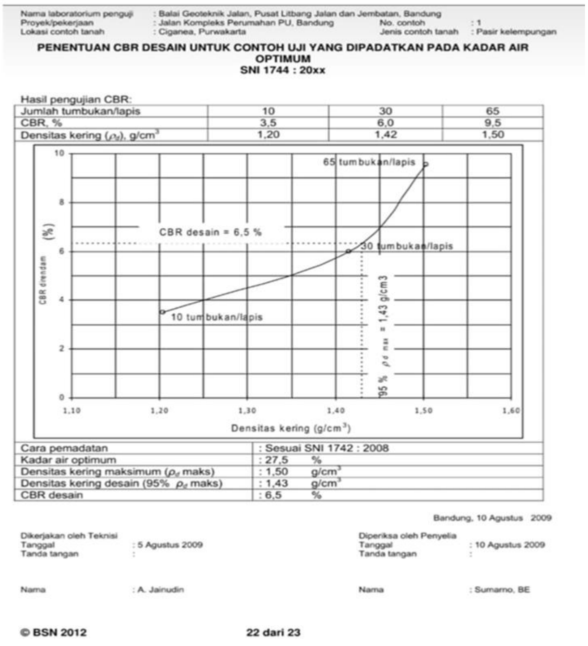

Nama laboratorium penguji : Balai Geoteknik Jalan, Pusat Litbang Jalan dan Jembatan, Bandung
Proyek/pekerjaan : Jalan Kompleks Perumahan PU, Bandung No. contoh : 1
Lokasi contoh tanah : Ciganea, Purwakarta Jenis contoh tanah : Pasir kelempungan

PENENTUAN CBR DESAIN UNTUK CONTOH UJI YANG DIPADATKAN PADA KADAR AIR OPTIMUM
SNI 1744 : 20xx

Hasil pengujian CBR:

Jumlah tumbukan/lapis	10	30	65
CBR, %	3,5	6,0	9,5
Densitas kering (ρ_d), g/cm^3	1,20	1,42	1,50

Cara pemadatan	: Sesuai SNI 1742 : 2008
Kadar air optimum	: 27,5 %
Densitas kering maksimum (ρ_d maks)	: 1,50 g/cm^3
Densitas kering desain (95% ρ_d maks)	: 1,43 g/cm^3
CBR desain	: 6,5 %

Bandung, 10 Agustus 2009

Dikerjakan oleh Teknisi
Tanggal : 5 Agustus 2009
Tanda tangan :
Nama : A. Jainudin

Diperiksa oleh Penyelia
Tanggal : 10 Agustus 2009
Tanda tangan :
Nama : Sumarno, BE

© BSN 2012 22 dari 23

Figure 2. Determination of CBR of heap land with red soil

1) A micro pile, 15 × 15 cm in cross-section, serves as the foundation for the MSE wall. The MSE Half panel system is then installed on the existing soil conditions (Figure 3).

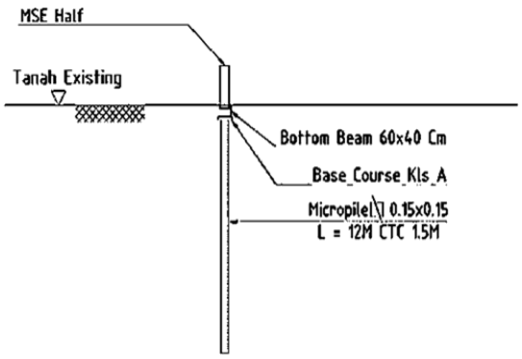

Figure 3. The MSE Half panel system installation

2) Anchors, Cross Necklaces, and Startails are installed within the MSE Half structure (Figure 4), with a 40 cm layer of red soil placed above.

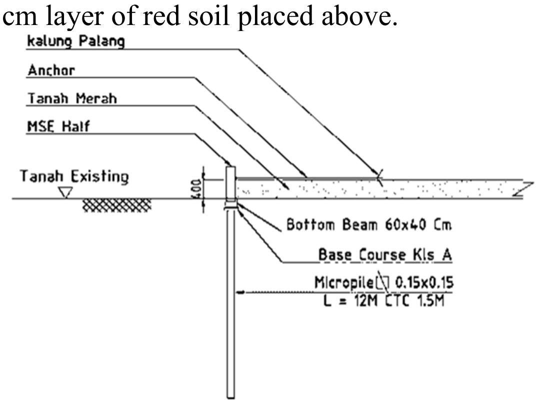

Figure 4. Installation of Anchors, Cross Necklaces, and Startails within the MSE Half panel system

3) Additional 40 cm layers of red soil are added and compacted using a vibratory roller to ensure interlock and stability between structural elements (Figure 5). This incremental placement and compaction enhance shear resistance and overall structural integrity, resulting in a robust MSE wall. The anchor length ranges from 0.5 to 0.7 times the wall height (H) and extends beyond the potential failure plane, inclined at an angle of 45° + φ/2, where φ is the soil's effective friction angle.

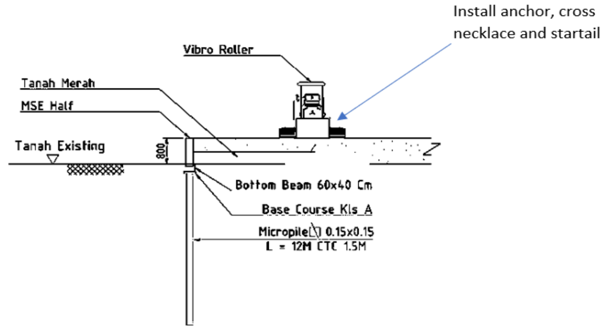

Figure 5. Vibratory roller operation

4) The second anchor was installed, followed by placement of an 80 cm layer of red soil, which was then compacted using a vibratory roller to ensure structural consolidation and interlock with the reinforcement (Figure 6).

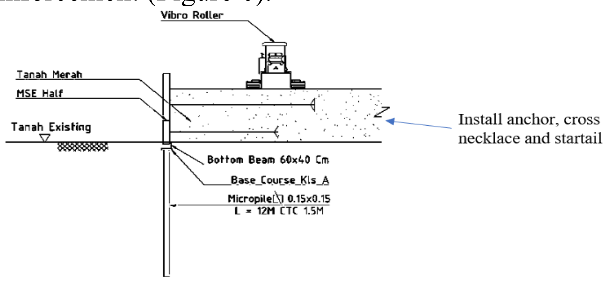

Figure 6. The second anchor installation

5) The third anchor was installed, followed by placement of a 120 cm layer of red soil, which was then compacted using a vibratory roller (Figure 7).

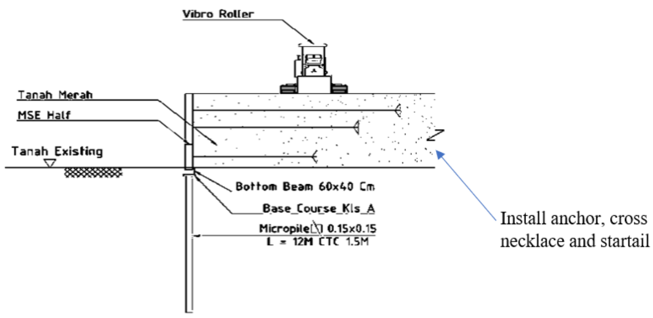

Figure 7. The third anchor installation

3. Results and Discussion

We evaluate external stability with respect to overturning, sliding, and foundation bearing capacity, in accordance with standard retaining wall practice. In this context, the performance of the MSE wall is governed by the following criteria:

- Resultant moments due to lateral earth and hydrostatic pressures are compared with stabilizing moments from self-weight, surcharge over the heel, and any additional permanent loads. Acceptable performance is indicated by a sufficient factor of safety against overturning and by a base resultant located within the middle third of the footing to avoid tensile stresses at the heel.
- Horizontal driving forces are resisted by base friction and any passive resistance mobilized at the toe (where permitted by the governing standard). Adequate performance is demonstrated when resisting forces exceed driving forces by the required safety margin.

The vertical resultant and its eccentricity determine the distribution of contact pressure beneath the base. The maximum computed pressure must remain below the allowable bearing capacity, and the pressure distribution must remain compressive across the entire effective base width to minimize differential settlement and rotation (see Appendix A).

Conclusion: The factor of safety for the Mechanically Stabilized Earth (MSE) wall complies with the requirements specified in SNI Geoteknik No. 8460:2017, which stipulates a minimum factor of safety of 1.5 for all stability checks. The results are summarized as follows:

a. Factor of Safety against Overturning (Sliding Stability Roll): 7.605 > 1.5 — OK

b. Factor of Safety against Sliding: 3.067 > 1.5 — OK

c. Factor of Safety against Bearing Capacity Failure: 10.482 > 1.5 — OK

d. Factor of Safety for Anchor Capacity: 5.72 > 1.5 — OK

All evaluated stability criteria are satisfied, confirming the structural adequacy of the design.

Note: Additional reference values for safety factors are based on [16].

3.1. Semi-Empirical Method

Ovesen and Stromann [17] proposed a semi-empirical method for determining the tensile capacity of the Cross Necklace and Anchor end. The calculation, performed in three steps, is as follows:

Step 1: Determine the embedment depth, H

Assume the anchor plate has a height of H and is continuous, with B (the length perpendicular to the cross-section) equal to x, as illustrated in the figure 8. The following notation is used:

P_p = Passive force per unit length of anchor

P_a = Active force per unit length of anchor

ϕ = Effective soil friction angle

δ = Friction angle between the anchor plate and the soil

P'_{ult} = Ultimate resistance per unit length of anchor

W = Effective weight per unit length of anchor plate

1) Finding the value of the active pressure coefficient (Ka)

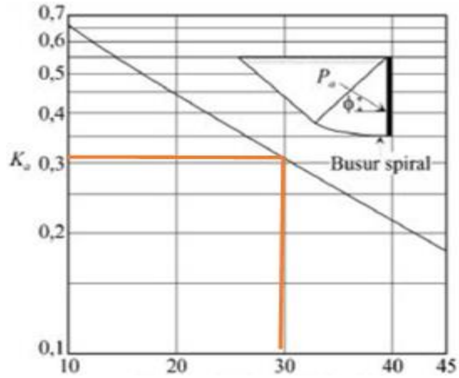

Figure 8. Ground friction angle, Φ (degree) Source: [16]

Ka = active pressure coefficient

Ka = 0.31

2) Finding effective weight values per unit length of anchor plate (W)

$$W = H\, t\, \gamma_{concrete}$$

W = 4.94 kN/m

3) Finding the value of the active pressure coefficient (K_p) (Figure 9).

$$K_p \sin\delta = \frac{W\ \tfrac{1}{2}\gamma H^2 K_a \sin\Phi}{\tfrac{1}{2}\gamma H^2}$$

$K_p \sin\delta$ = Passive pressure coefficient

$K_p \sin\delta = 0.20$

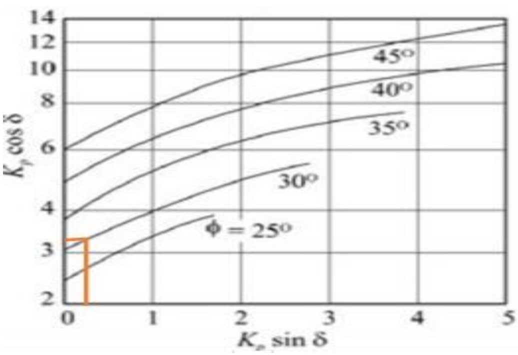

Figure 9. Determination of the active pressure coefficient. Source: [17]

$K_p \cos\delta = 3.30$

Step 2: Determine the actual height, H, of the anchor to be constructed

If a continuous anchor (i.e., an anchor with width B) of height h is installed in the soil at an embedment depth H, as illustrated in the figure above, the ultimate resistance per unit length is determined as follows:

4) Finding the ultimate resistance per unit length of the anchor (P'_{ult})

$$P'_{ult} = \tfrac{1}{2}\gamma H^2 K_p \cos\delta' - P_a \cos\phi' = \tfrac{1}{2}\gamma H^2 K_p \cos\delta' - \tfrac{1}{2}\gamma H^2 K_a$$
$$= \tfrac{1}{2}\gamma H^2 (K_p \cos\delta' - K_a \cos\phi')$$

P'_{ult} = ultimate resistance value per unit length of anchor
P'_{ult} = 306.56 kN/m

5) Finding the ultimate pullout resistance of the anchor plate (P'_{us})

$$P'_{us} = \left[\frac{C_{ov}+1}{C_{ov+}\left(\frac{H}{h}\right)}\right] P'_{ult}$$

To calculate P'_{us}, assume the red soil is cohesive. The soil cohesion value is given as:
c_{ov} = Soil cohesion coefficient = 14.00 kPa
Where:
P'_{us} = Ultimate pullout resistance per unit length of the anchor plate
P'_{us} = 123.17 kN/m

6) Finding the center-to-center spacing between anchors (S')*

The CTC spacing between anchors is defined as S':
30 cm = 0.3 m
50 cm = 0.5 m
100 cm = 1.0 m
150 cm = 1.5 m
200 cm = 2.0 m
250 cm = 2.5 m

7) Finding value S'-B/H+h
B = Anchor Box Width
H = Anchor box height with ground level
h = Anchor Box Height

30cm	=	0.04
50cm	=	0.10
100cm	=	0.23
150cm	=	0.37
200cm	=	0.51
250cm	=	0.64

7) Finding equivalent length values (B_e)
B_e-B/H-h = Derived from the Table

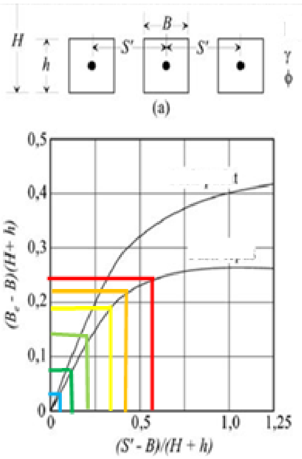

30cm	=	0.02
50cm	=	0.08
100cm	=	0.15
150cm	=	0.19
200cm	=	0.22
250cm	=	0.24

B_e	=	Equivalent length
30cm	=	0.04
50cm	=	0.10
100cm	=	0.23
150cm	=	0.37
200cm	=	0.51
250cm	=	0.64

9) Finding the ultimate voltage value (P'_{ult})

$$P'_{ult} = P'_{us} B_e$$

P'_{ult}	=	Ultimate Voltage	
30cm	=	19.15	kN
50cm	=	21.18	kN
100cm	=	23.54	kN
150cm	=	24.89	kN
200cm	=	25.90	kN
250cm	=	26.57	kN

10) Finding the allowable voltage value (P_{all})

$$P_{all} = \frac{P_{ult}}{FS}$$

P_{all}	=	Permitted voltage	
FS	=	Safety Factor	
30cm	=	9.58	kN
50cm	=	10.59	kN
100cm	=	11.77	kN
150cm	=	12.44	kN
200cm	=	12.95	kN
250cm	=	13.29	kN

11) Finding tensile strength values per unit length (F)

$$S' = \frac{P_{all}}{F}$$

F	=	tensile strength per unit length	
30cm	=	31.92	kN
50cm	=	21.18	kN
100cm	=	11.77	kN
150cm	=	8.30	kN
200cm	=	6.47	kN
250cm	=	5.37	kN

L = Anchor Length Value = 2.5 m (Assumption Value)
F = F x L

F (30cm)	=	79.79	kN
F (50cm)	=	52.94	kN
F (100cm)	=	29.42	kN
F (150cm)	=	20.74	kN
F (200cm)	=	16.19	kN
F (250cm)	=	13.29	kN

Therefore, it can be concluded from the calculations above that the smaller the center-to-center spacing between anchors (S'), the greater the tensile capacity (F).

3.2. Examination and Test Results Data

3.2.1. Workflow

The experimental study on anchors with Cross Necklaces and Startails was conducted in several stages, as follows:

a. Constructing the test tank and installing wire mesh reinforcement,

b. Casting of the retaining wall panels,

c. Backfilling, providing soil compaction, and installation of Cross Necklace anchor test specimens,

d. Testing tensile strength of Cross Necklace anchors.

3.2.2. Test Specimen Fabrication

The fabrication of the two test specimens involved constructing a concrete soil-retaining wall reinforced with M10 wire mesh and producing a Cross Necklace anchor specimen using plain iron bar of Ø19 mm diameter (Figures 10-11).

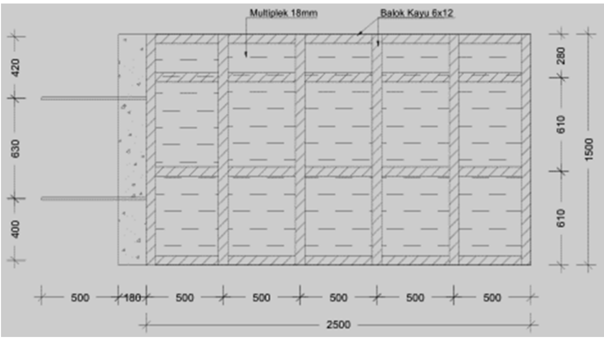

Figure 10. Side formwork sketch (designed by the authors)

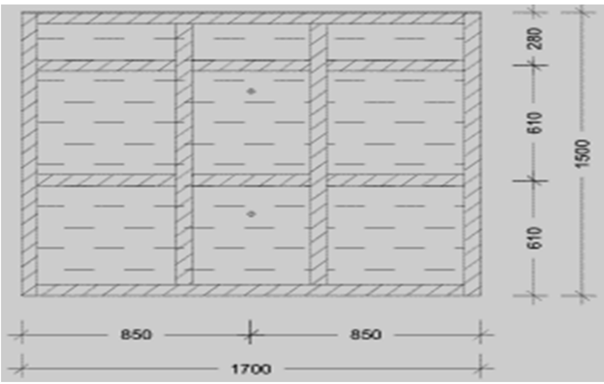

Figure 11. Front formwork sketch (designed by the authors)

3.2.3. Retaining Wall Casting Work

The casting of the soil-retaining wall was carried out using instant concrete materials with a target compressive strength corresponding to the K-500 grade.

The following is the mix design for K-500 concrete per 50 kg bag of cement:

a. Cement: 50.0 kg

b. Coarse aggregate (screen): 23.925 kg

c. Sand: 16.0 kg

d. Liquid admixture: 0.075 kg

3.2.4. Backfill and Compaction Work

The backfilling process involved placing soil in layers and installing the Cross Necklace anchor specimen.

Compaction was performed by tamping each 20 cm lift of soil using a vibratory plate compactor (stamper). The soil was maintained at a moist condition through regular water spraying to optimize compaction efficiency.

3.2.5. Cross Necklace Tensile Testing

Tensile testing of the Cross Necklace anchors was conducted in two stages:

a. Stage 1 Testing

b. Stage 2 Testing

Stage 1 Testing:

In the first stage, the Cross Necklace anchor was installed with a Startail configuration at the bottom (50 cm center-to-center, CTC, spacing) and a 30 cm CTC Cross Necklace configuration at the top (Figure 12).

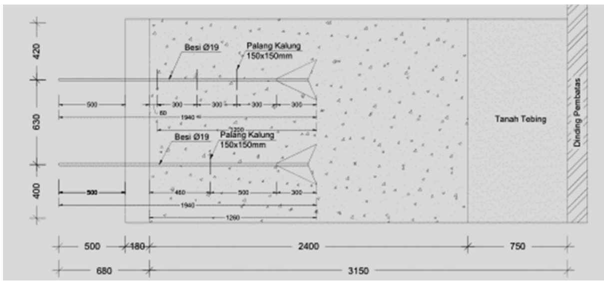

Figure 12. Stage 1 anchor iron installation scheme (designed by the authors)

Stage 2 Testing:

In the second stage, the configuration was reversed: a Startail with 50 cm CTC spacing was placed at the top, and a 30 cm CTC Cross Necklace was installed at the bottom (Figure 13).

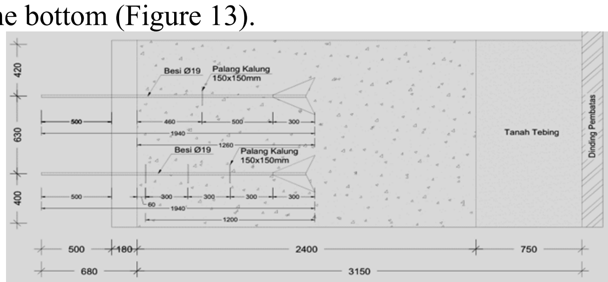

Figure 13. Stage 2 anchor iron installation scheme (designed by the authors)

On July 6, 2024, a pullout test was conducted on the anchor equipped with a Cross Necklace and a D19 Startail, which had been buried and compacted in the soil. The test was performed at two embedded anchor points, as indicated in the pullout test layout plan (Figure 14).

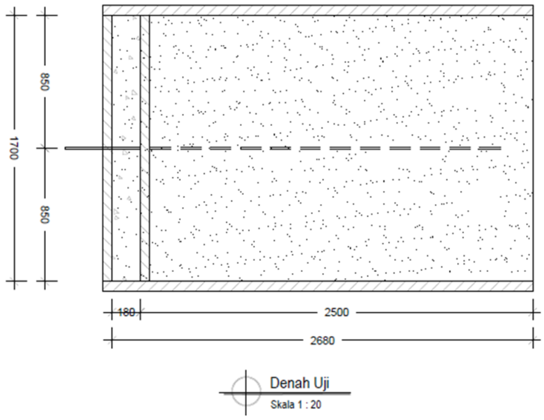

Figure 14. Test point plans (designed by the authors)

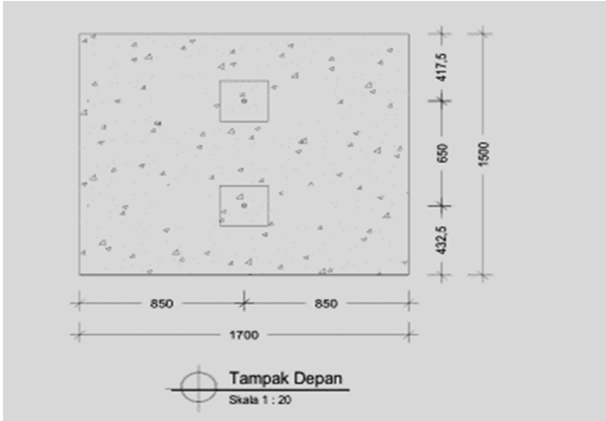

Figure 15. Front view of anchor location (designed by the authors)

On July 15, 2024, a second pullout test was carried out on an identical anchor configuration under the same installation and compaction conditions. The test layout plan shows the location of the two anchor points embedded in the backfill (Figure 15).

The results of the tensile strength tests on the Cross Necklace anchors revealed the following pullout capacities:

In Phase 1 Testing (Table 1):

Cross Necklace with 50 cm CTC spacing (lower anchor): 38.4 kN

Cross Necklace with 30 cm CTC spacing (upper anchor): 32.1 kN

Table 1. Results of the tensile test of the Cross Necklace anchor Phase 1 (compiled by the authors)

Load Test Summary							
Project Name			Anchor with Cross Necklace and Startail				
Testing Equipment			*Enerpac Rch 302 (Cylinder Effective Area 46.6 Cm²)*				
Base Material					*Type of Fastening System*		*Rebar D 19*
Compressive Strength					*Note*		
Test Result							
No	Anchor Detail	Date Of Test	Design Resistance [Kn]	Ultimate Resistance [Kn]	Recorded Test Load [Kn]	Remarks	Cross Distance
1.	Point No. 1 (1.200 Psi)	6-07-2024			38.4 Kn	Upper Anchor	CTC 50cm
2.	Point No. 2 (1.000 Psi)	6-07-2024			32.1 Kn	Lower Anchor	CTC 30cm

In Phase 2 Testing (Table 2):

Cross Necklace with 50 cm CTC spacing (upper anchor): 35.2 kN

Cross Necklace with 30 cm CTC spacing (lower anchor): 89.6 kN

Table 2. Results of the Phase 2 shutdown test (compiled by the authors)

Load Test Summary							
Project Name			Anchor with Cross Necklace and Startail				
Testing Equipment			*Enerpac Rch 302 (Cylinder Effective Area 46.6 Cm²)*				
Base Material					*Type of Fastening System*		*Rebar D 19*
Compressive Strength					*Note*		
Test Result							
No	Anchor Detail	Date Of Test	Design Resistance [Kn]	Ultimate Resistance [Kn]	Recorded Test Load [Kn]	Remarks	Cross Distance
1.	Point No. 1 (2.800 Psi)	15-07-2024			89.6 Kn	Upper Anchor	CTC 30cm
2.	Point No. 2 (1.100 Psi)	15-07-2024			35.2 Kn	Lower Anchor	CTC 50cm

These results indicate a significant increase in pullout resistance when the 30 cm CTC Cross Necklace is placed at the lower anchor position, suggesting that location and spacing configuration play a critical role in reinforcement performance.

3.3. Analysis and Discussion of Pull-Out Using PLAXIS 3D

3.3.1. Research Location

The research was conducted at Jl. Cijerokaso No. 67, Sarijadi Village, Sukasari District, Bandung City, West Java Province. This location was selected due to the presence of red soil with characteristics suitable for anchor pull-out testing. The soil conditions at the site enable the acquisition of representative and accurate data on anchor performance in typical red soil environments. The physical and geotechnical properties of the red soil contribute significantly to the validity and reliability of the research findings.

3.3.2. Data Processing

The data used in this research consists of correlation data derived from various reference sources. This correlated data forms a critical basis for the analysis, as each dataset plays an important role in characterizing soil behavior under anchor pull-out conditions. The correlation data was compiled from existing literature, including previous studies relevant to and closely aligned with the research topic.

Subsequently, the collected correlation data was processed and analyzed using PLAXIS 3D software. PLAXIS was selected as the primary analysis tool due to its proven capability in performing accurate and reliable geotechnical simulations. Inputting data into PLAXIS involved rigorous verification and validation procedures to ensure that the parameters used reflect actual field conditions and design specifications. Key input parameters include soil cohesion, effective internal friction angle, and modulus of elasticity; all were derived from the compiled correlation data.

The data processing workflow also includes model calibration to ensure that simulation results closely match field conditions. This step enhances the reliability and predictive accuracy of the numerical model. Thus, the use of correlation data from multiple sources provides a robust foundation for the geotechnical analysis and supports the validity of the simulation outcomes.

3.3.3. Soil Parameter Data

The field investigation data, including Standard Penetration Test (SPT) values (N-SPT), soil descriptions, groundwater table depth, and other geotechnical observations, were obtained from borehole logs (Drill Logs). These data were used to determine the in-situ soil parameters. Soil properties were derived through correlation methods, based on the N-SPT results and calibrated using established empirical relationships from multiple reference sources, as shown in Tables 3-7.

Table 3. Typical value for bulk and saturated unit weight [18]

Soils		Bulk unit weight (kN/m^3)		Saturated unit weight (kN/m^3)	
		Loose	Dense	Loose	Dense
Granular soils	Gravel	16.0	18.0	20.0	21.0
	Well-graded sand and gravel	19.0	21.0	21.5	23.0
	Coarse or medium sand	16.5	18.5	20.0	21.5
	Well-graded sand	18.0	21.0	20.5	22.5
	Fine or silty sand	17.0	19.0	20.0	21.5
	Rock fill	15.0	17.5	19.5	21.0
	Brick hardcore	13.0	17.5	16.5	19.0
	Slag fill	12.0	15.0	18.0	20.0
	Ash fill	6.5	10.0	13.0	15.0
Cohesive soils	Peat (high variability)	12.0		12.0	
	Organic clay	15.0		15.0	
	Soft clay	17.0		17.0	
	Firm clay	18.0		18.0	
	Stiff clay	19.0		19.0	
	Hard clay	20.0		20.0	
	Stiff or hard glacial clay	21.0		21.0	

Table 4. Void Ratio [19]

Type of soil	Void ratio, *e*
Loose uniform sand	0.8
Dense uniform sand	0.45
Loose angular-grained silty sand	0.65
Dense angular-grained silty sand	0.4
Stiff clay	0.6
Soft clay	0.9-1.4
Loess	0.9
Soft organic clay	2.5-3.2
Glacial till	0.3

Table 5. Permeability [20]

Soil behavior type	Soil permeability (m/s)
Sensitive fine grained	3×10^{-9} to 3×10^{-8}
Organic soils – peats	1×10^{-8} to 1×10^{-6}
Clays-clay to silty clay	1×10^{-10} to 1×10^{-7}
Silt mixtures: clayey silt to silty clay	3×10^{-9} to 1×10^{-7}
Sand mixtures: silty sand to sandy silt	1×10^{-7} to 1×10^{-5}
Sands: clean sands to silty sands	1×10^{-5} to 1×10^{-3}
Gravelly sand to sand	1×10^{-3} to 1
[a] Very stiff sand to clayey sand	1×10^{-8} to 1×10^{-6}
[a] Very stiff fine grained	1×10^{-9} to 1×10^{-7}

Note: [a] Over consolidated or cemented

Table 6. Modulus of Elasticity [21]

Type	Strength of soil	Elastic modulus, E (MPa)	
		Short term	Long term
Gravel	Loose	25-50	
	Medium	50-100	
	Dense	100-200	
Medium to coarse sand	Very loose	< 5	
	Loose	3-10	
	Medium dense	8-30	
	Dense	25-50	
	Very dense	40-100	
Fine sand	Loose	5-10	
	Medium	10-25	
	Dense	25-50	
Silt	Soft	< 10	< 8
	Stiff	10-20	8-15
	Hard	> 20	> 15
Clay	Very soft	< 3	< 2
	Soft	2-7	1-5
	Firm	5-12	4-8
	Stiff	10-25	7-20
	Very stiff	20-50	15-35
	Hard	40-80	30-60

Table 7. Values of c' and *phi* [20]

Soil group	Typical soils in group	Soil parameters	
		$\acute{c}$ (kPa)	φ (degrees)
Poor	Soft and firm clay of medium to high plasticity; silty clays; loose variable clayey fills, loose sandy silts	0-5	17-25
Average	Stiff sandy clays; gravelly clays; compact clayey sands and sandy silts; compacted clay fills	0-10	26-32
Good	Gravelly sands, compacted sands, controlled sandstone and graveled fills, dense well graded sands	0-5	32-37
Very good	Weak weathered rock, controlled fills of road base, gravel and recycled concrete	0=25	36-43

3.3.4. Structural Element Parameter Data

The structural element parameters include data for micro piles, plates, and soil clusters. Summary parameters for the structural elements to be modelled are presented in Tables 8-10.

Table 8. Data parameter micro pile (compiled by the authors)

Parameter	Information	Unit
Material Type	Embedded Beans	-
Specific gravity (γ)	24	kN/m^3
Modulus of Elasticity (E)	29988615	kN/m^2
Diameter	0.15	m

a. Assumption

Specific gravity of concrete (γ_{beton}) = 24 kN/m^3

b. Concrete Quality

$$K\text{-}500 = K \times 0{,}83 \times \frac{9{,}81}{100} = 500 \times 0{,}83 \times \frac{9{,}81}{100}$$

$F'c = 40.7115$ MPa

$$E = 4700\sqrt{f'c} = 4700\sqrt{40{,}7115}$$

$$= 29988.615 \; N/mm^2$$

$$E \approx 29.99 \times 10^6 \; kN/m^2$$

Table 9. Data parameter plate (compiled by the authors)

Property	Information	Unit
Capping Beam		
Material Type	Elastic	-
Specific Gravity (γ)	24	kN/m^3
Axial Stiffness (EA)	200.000	kN
Diameter	0.13	m
MSE Wall		
Material Type	Elastic	-
Specific Gravity (γ)	24	kN/m^3
Concrete Quality	K-500	-
Modulus of Elasticity (E)	29988615	kN/m^2
Diameter	0.18	m

Table 10. Data parameter soil cluster (compiled by the authors)

Property	Information	Unit
Anchor, Startail & Cross Necklace		
Soil Model	Linear Elastic	-
Drainage Type	Non-porous	-
Specific Gravity (γ)	78.50	kN/m^3
E_{ref}	100000000	kN/m^2
Poisson Rasio (v)	0.2	-
R_{inter}	0.750	-

3.4. Pull-Out Analysis Using PLAXIS 3D Software

The numerical model developed in PLAXIS 3D was geometrically calibrated to match the field test conditions. This calibration included the dimensions and configuration of the red soil, as well as the position and orientation of the anchor. Each geometric detail was carefully defined to ensure that the model accurately represents the actual conditions at the research site. This approach enhances the reliability of the simulations and ensures that the results are representative of real-world behavior.

The pull-out testing sequence was also replicated in the simulation to reflect the field procedures. The test began with the lower anchor, which had a CTC spacing of 30 cm. A tensile force was gradually applied until the anchor reached its ultimate pull-out capacity. The data obtained from this stage were used to validate the numerical model and verify that the soil's response to loading aligned with expected geotechnical behavior.

After the pull-out test on the first anchor was completed, the procedure proceeded to the second anchor, which had a CTC spacing of 50 cm. The same testing method was applied to ensure consistent tensile loading, enabling a direct comparison between the results obtained from the two anchors. Each test stage was designed to provide clear insight into the response of red soil to the applied tensile forces.

The results of the pull-out simulation using PLAXIS 3D were analyzed to gain a deeper understanding of the soil–anchor interaction behavior. The distribution of stress and strain around the anchors, soil deformation patterns, and the interaction mechanisms between the anchors and red soil were thoroughly evaluated. These simulation results provide valuable insights into load transfer mechanisms and potential failure modes within the anchor system in red soil. This analysis helps identify key factors influencing anchor performance and supports recommendations for design optimization and improved construction practices. The backfill soil parameters used in the PLAXIS 3D model were based on the red soil properties derived from empirical correlations and field data.

With geometric adjustments and test sequences closely replicating field conditions, numerical modelling using PLAXIS 3D provides a comprehensive and realistic approach to analyzing anchor performance in red soil. The results of this analysis enhance both theoretical understanding and practical insight, offering actionable guidance for geotechnical projects involving anchors in similar soil conditions. In addition to field pull-out testing, numerical simulations were conducted using PLAXIS 3D to complement and validate the experimental findings. The geometric configuration of the pull-out model is illustrated in Figure 16.

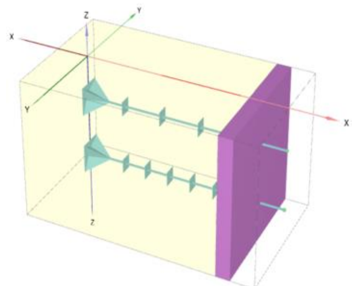

Figure 16. Geometry of pull-out modeling (designed by the authors)

Based on Figure 16, anchor 1 has a spacing of 50 cm, while anchor 2 has a spacing of 30 cm. In the field testing, anchor no. 2 was pulled first, followed by anchor no. 1. This sequence was replicated in the PLAXIS 3D analysis, where the pull-out simulation was conducted in the same order: anchor no. 2 first, followed by anchor no. 1.

3.4.1. Pull-Out Analysis Results Using PLAXIS 3D Software

The pull-out analysis performed in PLAXIS 3D revealed variations in anchor capacity depending on the CTC spacing. For the anchor with a 30 cm CTC spacing, the simulated tensile capacity was 87.9 kN. This result indicates that at closer spacing, the interaction between the anchor and red soil is significantly enhanced, enabling the system to develop higher pull-out resistance. Analysis of the stress and strain distribution around the anchor showed a high concentration of stress at the anchor–soil interface, indicating that the red soil effectively mobilizes shear resistance and sustains tensile loads at this CTC distance.

In contrast, the results for anchors with a 50 cm CTC spacing showed a lower tensile capacity of 45.2 kN. This reduction in capacity can be attributed to decreased soil–anchor interaction and a more uniform distribution of stress around the anchor. At larger spacings, the red soil may not provide sufficient confinement, resulting in lower tensile resistance compared to the 30 cm CTC configuration. These findings are critical for the design and installation of anchors in the field, particularly in determining the optimal spacing to maximize pull-out capacity.

The comparison of pull-out results between the 30 cm and 50 cm CTC configurations provides valuable insights into how anchor spacing influences anchor performance in red soil. Further analysis of the simulation results revealed that at 30 cm spacing, the proximity of anchors affects load distribution and soil deformation, indicating a degree of interaction between adjacent elements. In contrast, at 50 cm spacing, anchors behave more independently, with minimal interaction, but exhibit lower overall tensile capacity.

These results demonstrate that the selection of anchor spacing is a critical factor in optimizing anchor system design. The higher tensile capacity observed at a 30 cm spacing indicates that, under the tested conditions, closer spacing enhances the efficiency of the anchor–soil system. However, other factors must also be considered, such as potential interference during installation and the overall stability of the reinforced structure.

Therefore, the findings of this analysis provide a robust basis for practical recommendations in the design and installation of anchors in geotechnical projects, particularly in red soil conditions. The pull-out test results obtained from the PLAXIS 3D simulations are presented in Figure 17.

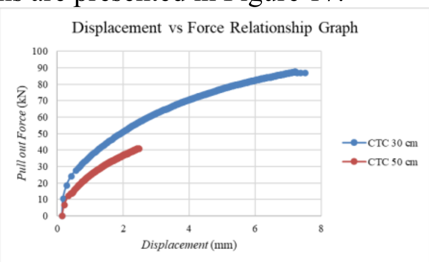

Figure 17. Graph of the relationship of displacement to force (designed by the authors)

Based on the graph presented in Figure 17, the pull-out-to-failure load for the 30 cm CTC spacing was 87.9 kN, while the pull-out capacity for the 50 cm CTC spacing was 45.21 kN.

3.5. Case Study Analysis and Discussion

3.5.1. Background

Soil retaining walls are critical components in infrastructure construction, particularly in areas with unstable or weak soil conditions [22]. Mechanically Stabilized Earth (MSE) walls have emerged as a widely adopted solution for addressing these challenges. The model developed in this study integrates two innovative reinforcement systems ("Cross Necklace" and "Fish Fin Startail") specifically designed to enhance the stability and load-bearing capacity of MSE walls in challenging red soil conditions.

Red soil, characterized by high plasticity, low bearing capacity, and susceptibility to swelling and shrinkage, presents significant geotechnical challenges in MSE wall construction. These properties can lead to increased lateral pressures, differential settlement, and reduced anchorage performance, necessitating advanced reinforcement strategies to ensure long-term structural integrity.

3.5.2. Case Study Location

The case study was conducted in Jatireja, East Cikarang, West Java, specifically at the Jababeka IX Industrial Estate Bridge Construction project. This location was selected due to constrained right-of-way (ROW) conditions, necessitating an efficient soil-retaining wall solution in terms of both space utilization and cost-effectiveness.

The Mechanically Stabilized Earth (MSE) wall, incorporating the Cross Necklace and Fish Fin Startail reinforcement system, was chosen as the optimal solution to address soil stability challenges at the site. Geologically, the subsurface conditions at Jababeka IX consist of brown silty clay, with consistency ranging from soft to very stiff.

3.5.3. Design Criteria

According to SNI 8460:2017 on Geotechnical Design Requirements, the maximum allowable horizontal displacement during construction for Mechanically Stabilized Earth (MSE) walls is approximately H/250 for rigid reinforcement and H/75 for flexible reinforcement. The resulting slope due to differential horizontal movement between the base and the top of the wall should be less than 4 mm/m of wall height. Post-construction horizontal movement is expected to be negligible.

In this case study, flexible reinforcement is used; therefore, the applicable criterion is H/75, where H is the height of the MSE wall. Given a wall height of 5.25 m, the allowable horizontal displacement was calculated as 0.07 m (70 mm).

In addition to displacement limits, the MSE wall design was evaluated against global safety factor criteria based on SNI 8460:2017, which specifies minimum factors of safety for four potential external failure modes as shown in Table 11.

Table 11. Summary of the minimum safety factors for the four potential external failures (compiled by the authors)

No.	Potential External Failure	Minimum Safety Factor (FK)	Other requirements	Repair Steps if FK is not Fulfilled
1	Lateral slide on the base	1.5	-	Extend L
2	Stylistic resultant eccentricity (rolling moment)	2 (roll)	e ≤ L/6	Extend L
3	Bearing capacity	2.5	-	Repair the soil Foundation or deepen D_m
4	Global stability	1.3	-	Extend the L or fix the foundation soil
Information				
L is the length of the reinforcement				
e is the resultant eccentricity of the forces				

3.5.4. Case Study Modeling Analysis with PLAXIS 3D

The numerical modelling performed using PLAXIS 3D in this case study provides valuable insights into anchor behavior in red soil. Through detailed simulations, PLAXIS 3D effectively captures the complex three-dimensional interactions between anchors and soil, closely replicating actual field conditions.

The anchors installed in the field were modelled in PLAXIS 3D with precise attention to their position and orientation as specified in the working drawings. Each anchor was positioned at a predetermined depth, with varying CTC spacing.

In this study, three modelling scenarios were developed using PLAXIS 3D to evaluate the influence of anchor spacing (CTC) on tensile capacity in red soil. The configurations analyzed included CTC spacings of 30 cm, 50 cm, and 70 cm. Each variation provides critical insight into how anchor spacing affects the distribution of maximum stress, strain, and achievable tensile capacity in red soil.

3.5.5. Modeling Geometry

The modelling process begins with defining the soil geometry based on the stratigraphic profile of the red soil layer at the research site. According to the field working drawings, the dimensions and thickness of the red soil layer are accurately input into PLAXIS 3D. The soil model incorporates layer conditions derived from borehole logs and local geotechnical data, reflecting spatial variability in soil properties across the study area. The geometry is carefully structured to ensure accurate representation of the entire zone influenced by the anchor.

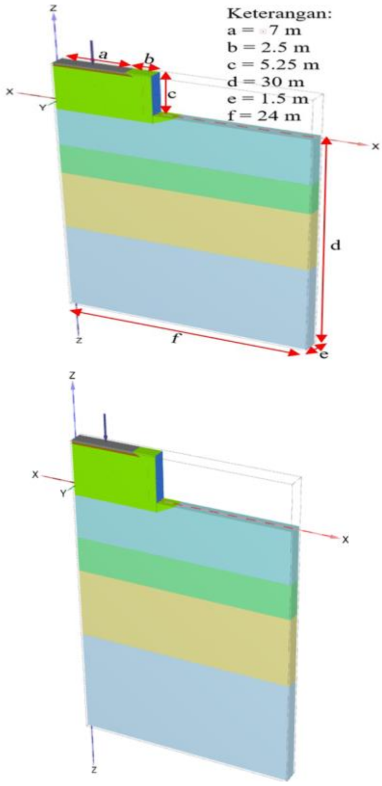

Figure 18. Modeling geometry (designed by the authors)

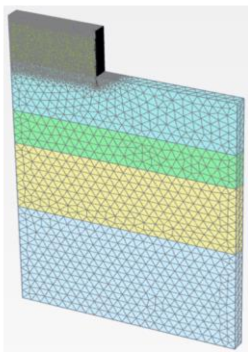

Figure 19. Meshing modeling results (designed by the authors)

3.5.6. Construction Stages

The PLAXIS 3D model employs a half-model geometry approach to simplify the computational process. The simulation was conducted in multiple construction stages, comprising three excavation phases and 16 backfilling stages, including the final construction phase and the installation of anchors.

The model has a total height of 5.25 m, with anchor spacing set at 0.5 m between the first and second anchors, and 1.0 m between the second and third anchors, continuing at 1.0 m intervals up to the seventh anchor. In the final construction stage, all components, including the road pavement, were fully implemented.

The modelling also includes an operational phase of one year, during which the structure is subjected to a traffic load of 15 kPa. Additionally, a 10-year operational stage was simulated, assuming sustained traffic loading under the same traffic loading conditions.

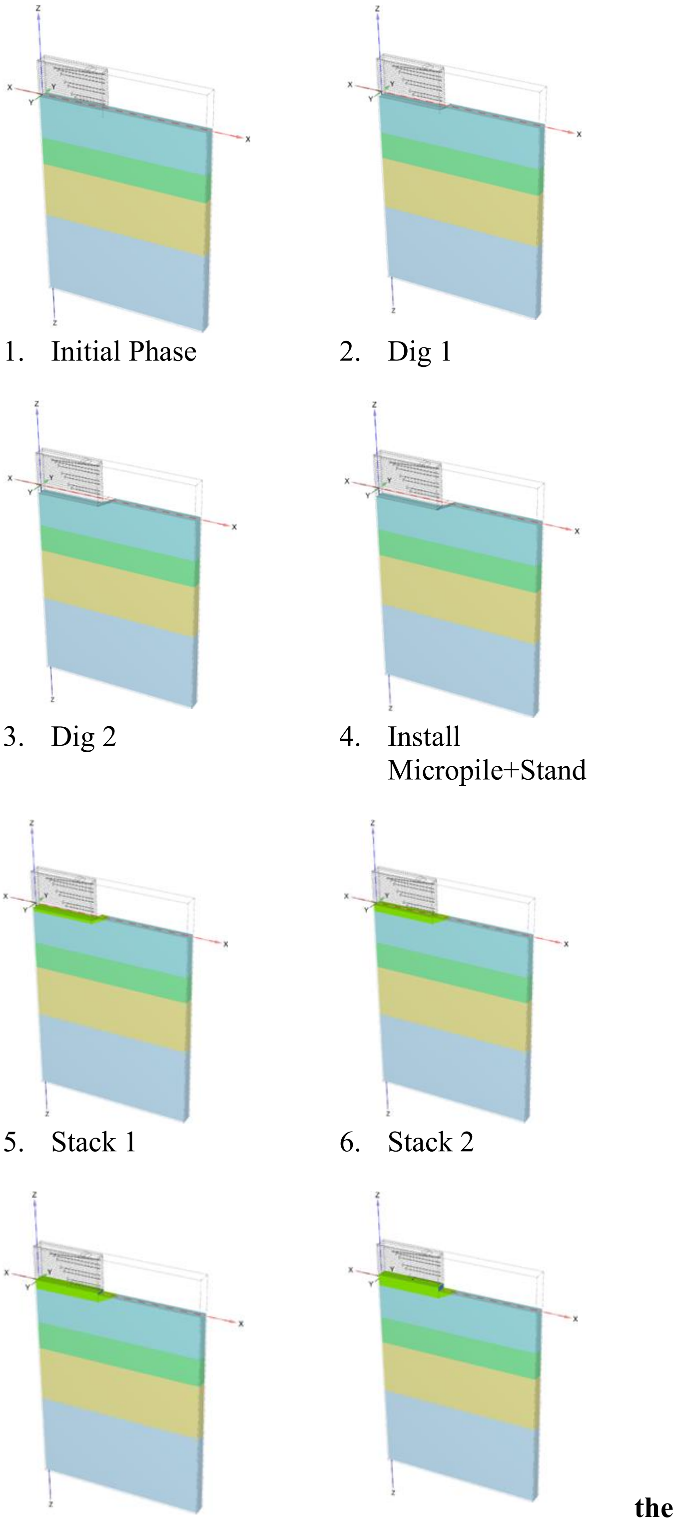

1. Initial Phase
2. Dig 1
3. Dig 2
4. Install Micropile+Stand
5. Stack 1
6. Stack 2

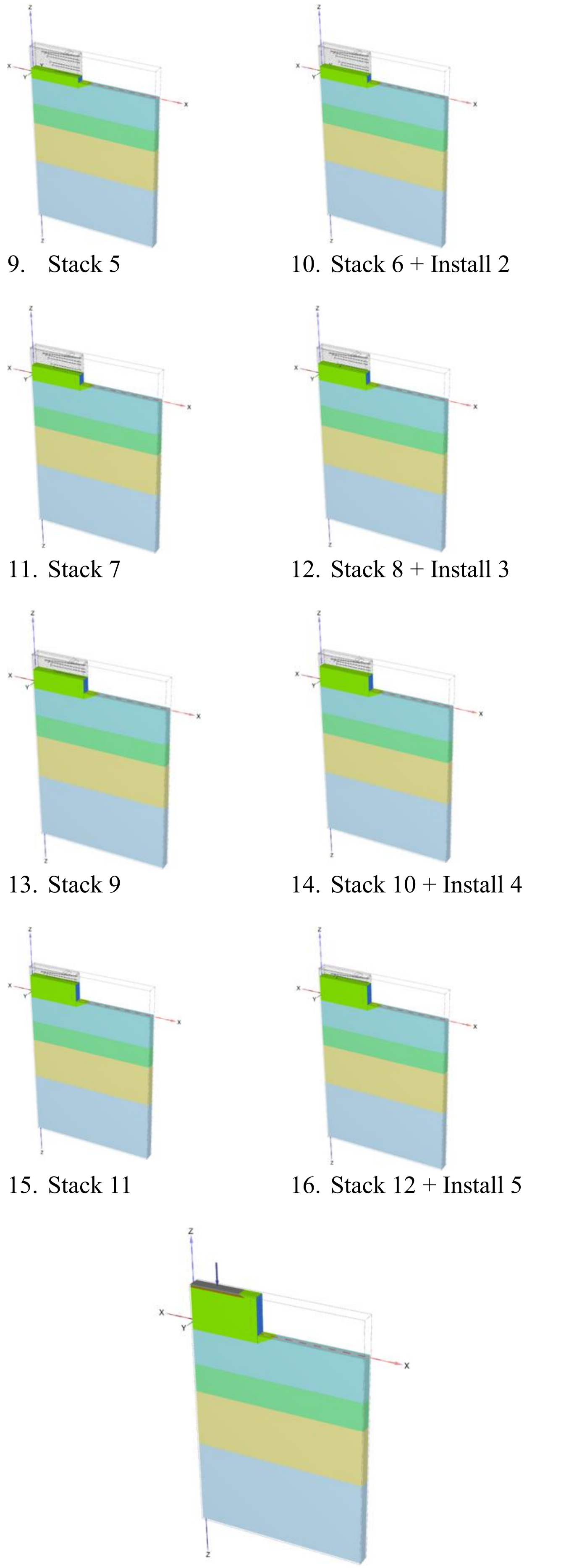

7. Stack 3
8. Stack 4 + Install 1
9. Stack 5
10. Stack 6 + Install 2
11. Stack 7
12. Stack 8 + Install 3
13. Stack 9
14. Stack 10 + Install 4
15. Stack 11
16. Stack 12 + Install 5

Figure 20. Soil geometry and statistics (designed by the authors)

Furthermore, the anchors installed in the field were modelled in PLAXIS 3D with precise attention to their position and orientation as specified in the working drawings. Each anchor was placed at a predetermined depth, with varying CTC spacing of 30 cm, 50 cm, and 70 cm. This geometric configuration is critical to accurately capture the stress distribution and soil deformation induced by tensile loading. Within the model, each anchor was assigned appropriate material properties to reflect the tensile strength and stiffness defined in the design specifications.

Micro pile 12 m

MSE Wall K500

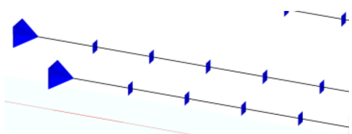

Anchor (f 19mm), Fish Fin (300mm x 300mm), and Cross Necklace (100x65mm t=6mm)

Figure 21. Anchor Details with modified Cross Necklace and Fish Fin models (developed by the authors)

3.5.7. *Results of Case Study Modeling Analysis Using 3D PLAXIS*

In this study, eleven modelling scenarios were developed using PLAXIS 3D to evaluate the influence of CTC spacing on anchor tensile capacity in red soil. The configurations analyzed are as follows:

1) Cross Necklace 15 cm × 15 cm, CTC 30 cm, with Anchor and Startail
2) Cross Necklace 15 cm × 15 cm, CTC 50 cm, with Anchor and Startail
3) Cross Necklace 15 cm × 15 cm, CTC 70 cm, with Anchor and Startail
4) Cross Necklace 15 cm × 15 cm, CTC 30 cm, without Startail
5) Cross Necklace 30 cm × 30 cm, CTC 30 cm, without Startail
6) Cross Necklace 40 cm × 40 cm, CTC 30 cm, without Startail
7) Anchor and Startail, without Cross Necklace
8) Cross Necklace 30 cm × 30 cm, CTC 30 cm, with Anchor and Startail
9) Cross Necklace 30 cm × 30 cm, CTC 50 cm, with Anchor and Startail
10) Cross Necklace 30 cm × 30 cm, CTC 70 cm, with Anchor and Startail
11) Anchor only, without Cross Necklace and Startail.

Each of these variations provides valuable insights into how anchor spacing influences the distribution of maximum stress, strain, and achievable tensile capacity in red soil.

Analysis Results: Startail, Anchor, Cross Necklace 15 cm × 15 cm, CTC 30 cm

PLAXIS 3D modelling with a 30 cm center-to-center (CTC) spacing yielded significant findings regarding the distribution of stress, strain, and deformation in red soil. In this configuration, the interaction between the anchor and the surrounding soil is highly intensified, with a pronounced concentration of stress around the anchor. This high stress zone indicates that the red soil provides strong confinement and support, enabling the anchor to resist substantial tensile forces.

The summary of the modelling results for the Startail, Anchor, and Cross Necklace (15 cm × 15 cm, CTC 30 cm) is presented in Table 12.

The reported values correspond to the maximum deformation observed in the wall facing or MSE structure.

Table 12. The summary of analysis results for modelling scenario 1 (compiled by the authors)

No	Construction Stages	Horizontal Facing Deformation (Ux) (mm)	SF
1	Put on MSE, Stack, Put Anchor 1	6.119	5.400
2	Put on MSE, Stack, Put Anchor 2	10.59	4.420
3	Put on MSE, Stack, Put Anchor 3	20.98	3.030
4	Put on MSE, Stack, Put Anchor 4	25.51	2.480
5	Put on MSE, Stack, Put Anchor 5	36.41	2.150
6	Put on MSE, Stack, Put Anchor 6	40.79	1.920
7	Put on MSE, Stack, Put Anchor 7	41.21	1.730

8	Final Construction	43.55	1.600
9	1 year operational	58.08	1.580
10	10 years operational	58.11	1.670

Analysis Results: Startail, Anchor, Cross Necklace 15cm x 15cm (CTC 50cm)

The summary of the modelling results for the Startail, Anchor, and Cross Necklace (15 cm × 15 cm, CTC 50 cm) is presented in Table 13.

Table 13. The summary of analysis results for modelling scenario 2 (compiled by the authors)

No	Construction Stages	Horizontal Facing Deformation (Ux) (mm)	SF
1	Put on MSE, Stack, Put Anchor 1	6.408	6.559
2	Put on MSE, Stack, Put Anchor 2	11.07	3.843
3	Put on MSE, Stack, Put Anchor 3	20.65	2.514
4	Put on MSE, Stack, Put Anchor 4	25.59	2.098
5	Put on MSE, Stack, Put Anchor 5	37.01	1.911
6	Put on MSE, Stack, Put Anchor 6	42.57	1.540
7	Put on MSE, Stack, Put Anchor 7	43.14	1.566
8	Final Construction	44.45	1.524
9	1 year operational	59.49	1.563
10	10 years operational	59.51	1.568

The reported values correspond to the maximum deformation observed in the wall facing or MSE structure.

Analysis Results: Startail, Anchor, Cross Necklace 15cm x 15cm (CTC 70 cm)

The summary of the PLAXIS 3D modelling results for the Startail, Anchor, and Cross Necklace (15 cm × 15 cm, CTC 70 cm) is presented in Table 14.

Table 14. The summary of analysis results for modelling scenario 3 (compiled by the authors)

No	Construction Stages	Horizontal Facing Deformation (Ux) (mm)	SF
1	Put on MSE, Stack, Put Anchor 1	5.606	6.620
2	Put on MSE, Stack, Put Anchor 2	10.21	3.816
3	Put on MSE, Stack, Put Anchor 3	14.29	2.529
4	Put on MSE, Stack, Put Anchor 4	19.23	2.094
5	Put on MSE, Stack, Put Anchor 5	27.13	1.909
6	Put on MSE, Stack, Put Anchor 6	34.32	1.540
7	Put on MSE, Stack, Put Anchor 7	37.56	1.560
8	Final Construction	44.59	1.542
9	1 year operational	59.67	1.521
10	10 years operational	59.72	1.516

The reported values correspond to the maximum deformation observed in the wall facing or MSE structure.

Analysis Results: Anchor and Cross Necklace 15cm x 15cm CTC 30cm without Startail

PLAXIS 3D modelling of the anchor and Cross Necklace (15 cm × 15 cm, CTC 30 cm) without Startail yielded significant insights into the distribution of stress, strain, and deformation in red soil. In this configuration, the interaction between the anchor and surrounding soil is highly intensified, with a pronounced concentration of stress around the anchor. This high-stress zone indicates that the red soil provides substantial confinement and support, enabling the anchor to resist significant tensile forces.

The summary of the modelling results for the Anchor, and Cross Necklace (15 cm × 15 cm, CTC 30 cm) without Startail is presented in Table 15.

Table 15. The summary of analysis results for modelling scenario 4 (compiled by the authors)

No	Construction Stages	Horizontal Facing Deformation (Ux) (mm)	SF
1	Put on MSE, Stack, Put Anchor 1	6.577	6.944
2	Put on MSE, Stack, Put Anchor 2	12.02	4.491
3	Put on MSE, Stack, Put Anchor 3	25.68	2.971
4	Put on MSE, Stack, Put Anchor 4	34.24	2.565
5	Put on MSE, Stack, Put Anchor 5	41.03	2.13
6	Put on MSE, Stack, Put Anchor 6	44.45	1.886

7	Put on MSE, Stack, Put Anchor 7	48.45	1.707
8	Final Construction	52.97	1.668
9	1 year operational	68.13	1.563
10	10 years operational	68.17	1.624

The reported values correspond to the maximum deformation observed in the wall facing or MSE structure.

Analysis Results: Anchor and Cross Necklace 30 cm x 30 cm CTC 30 cm, without Startail

The summary of the PLAXIS 3D modelling results for the Anchor, and Cross Necklace (30 cm × 30 cm, CTC 30 cm) without Startail is presented in Table 16.

Table 16. The summary of analysis results for modelling scenario 5 (compiled by the authors)

No	Construction Stages	Horizontal Facing Deformation (Ux) (mm)	SF
1	Put on MSE, Stack, Put Anchor 1	5.447	4.354
2	Put on MSE, Stack, Put Anchor 2	10.69	3.89
3	Put on MSE, Stack, Put Anchor 3	15.4	2.635
4	Put on MSE, Stack, Put Anchor 4	19.12	2.277
5	Put on MSE, Stack, Put Anchor 5	32.01	1.952
6	Put on MSE, Stack, Put Anchor 6	42.68	1.723
7	Put on MSE, Stack, Put Anchor 7	56.08	1.685
8	Final Construction	56.2	1.612
9	1 year operational	64.06	1.537
10	10 years operational	65.84	1.531

The reported values correspond to the maximum deformation observed in the wall facing or MSE structure.

Analysis Results: Anchor and Cross Necklace 40 cm x 40 cm CTC 30 cm, without Startail

The summary of the PLAXIS 3D modelling results for the Anchor, and Cross Necklace (40 cm × 40 cm, CTC 30 cm) without Startail is presented in Table 17.

Table 17. The summary of analysis results for modelling scenario 6 (compiled by the authors)

No	Construction Stages	Horizontal Facing Deformation (Ux) (mm)	SF
1	Put on MSE, Stack, Put Anchor 1	5.421	7.655
2	Put on MSE, Stack, Put Anchor 2	10.69	4.417
3	Put on MSE, Stack, Put Anchor 3	21.94	3.835
4	Put on MSE, Stack, Put Anchor 4	29.58	3.11
5	Put on MSE, Stack, Put Anchor 5	40.08	2.424
6	Put on MSE, Stack, Put Anchor 6	48.24	1.891
7	Put on MSE, Stack, Put Anchor 7	54.07	1.837
8	Final Construction	59.34	1.791
9	1 year operational	62.26	1.687
10	10 years operational	62.26	1.533

The reported values correspond to the maximum deformation observed in the wall facing or MSE structure.

Analysis Results: Anchor and Startail (without Cross Necklace)

This time PLAXIS 3D modeling refers only to Startail and Anchor without a Cross Necklace. This modeling aims to determine the effect if the Cross Necklace is removed.

The summary of the PLAXIS 3D modelling results for the Startail and Anchor, without Cross Necklace is presented in Table 18.

Table 18. The summary of analysis results for modelling scenario 7 (compiled by the authors)

No	Construction Stages	Horizontal Facing Deformation (Ux) (mm)	SF
1	Put on MSE, Stack, Put Anchor 1	6.212	6.385
2	Put on MSE, Stack, Put Anchor 2	10.8	4.4
3	Put on MSE, Stack, Put Anchor 3	20.19	2.957
4	Put on MSE, Stack, Put Anchor 4	25.27	2.604
5	Put on MSE, Stack, Put Anchor 5	59.06	2.088
6	Put on MSE, Stack, Put Anchor 6	58.39	1.86

7	Put on MSE, Stack, Put Anchor 7	58.74	1.722
8	Final Construction	60.17	1.687
9	1 year operational	67.98	1.62
10	10 years operational	68.09	1.514

The reported values correspond to the maximum deformation observed in the wall facing or MSE structure.

Analysis Results: Startail, Anchor, Cross Necklace 30 cm x 30 cm (CTC 30 cm)

PLAXIS 3D modelling of the Startail, Anchor, and Cross Necklace (30 cm × 30 cm, CTC 30 cm) yielded significant insights into the distribution of stress, strain, and deformation in red soil. In this configuration, the interaction between the anchor and surrounding soil is highly intensified, with a pronounced concentration of stress around the anchor. This high-stress zone indicates that the red soil provides substantial confinement and support, enabling the anchor to resist significant tensile forces.

The summary of the modelling results for the Startail, Anchor, and Cross Necklace (30 cm × 30 cm, CTC 30 cm) is presented in Table 19.

Table 19. The summary of analysis results for modelling scenario 8 (compiled by the authors)

No	Construction Stages	Horizontal Facing Deformation (Ux) (mm)	SF
1	Put on MSE, Stack, Put Anchor 1	7.625	4.473
2	Put on MSE, Stack, Put Anchor 2	12.16	4.198
3	Put on MSE, Stack, Put Anchor 3	14.43	2.728
4	Put on MSE, Stack, Put Anchor 4	15.03	2.432
5	Put on MSE, Stack, Put Anchor 5	12.32	1.984
6	Put on MSE, Stack, Put Anchor 6	10.31	1.751
7	Put on MSE, Stack, Put Anchor 7	15.59	1.726
8	Final Construction	20.10	1.711
9	1 year operational	30.47	1.682
10	10 years operational	30.50	1.673

The reported values correspond to the maximum deformation observed in the wall facing or MSE structure.

Analysis Results: Startail, Anchor, Cross Necklace 30 cm x 30 cm (CTC 50 cm)

The summary of the modelling results for the Startail, Anchor, and Cross Necklace (30 cm × 30 cm, CTC 50 cm) is presented in Table 20.

Table 20. The summary of analysis results for modelling scenario 9 (compiled by the authors)

No	Construction Stages	Horizontal Facing Deformation (Ux) (mm)	SF
1	Put on MSE, Stack, Put Anchor 1	7.612	4.473
2	Put on MSE, Stack, Put Anchor 2	12.13	4.198
3	Put on MSE, Stack, Put Anchor 3	13.31	2.728
4	Put on MSE, Stack, Put Anchor 4	14.17	2.432
5	Put on MSE, Stack, Put Anchor 5	11.48	1.984
6	Put on MSE, Stack, Put Anchor 6	9.923	1.866
7	Put on MSE, Stack, Put Anchor 7	10.31	1.753
8	Final Construction	20.22	1.697
9	1 year operational	35.25	1.648
10	10 years operational	35.25	1.641

The reported values correspond to the maximum deformation observed in the wall facing or MSE structure.

Analysis Results: Startail, Anchor, Cross Necklace 30 cm x 30 cm (CTC 70 cm)

The summary of the modelling results for the Startail, Anchor, and Cross Necklace (30 cm × 30 cm, CTC 70 cm) is presented in Table 21.

Table 21. The summary of analysis results for modelling scenario 10 (compiled by the authors)

No	Construction Stages	Horizontal Facing Deformation (Ux) (mm)	SF
1	Put on MSE, Stack, Put Anchor 1	7.203	3.365
2	Put on MSE, Stack, Put Anchor 2	9.060	3.074
3	Put on MSE, Stack, Put Anchor 3	9.745	2.629

4	Put on MSE, Stack, Put Anchor 4	12.16	2.436
5	Put on MSE, Stack, Put Anchor 5	15.61	1.945
6	Put on MSE, Stack, Put Anchor 6	20.22	1.749
7	Put on MSE, Stack, Put Anchor 7	30.02	1.660
8	Final Construction	35.15	1.635
9	1 year operational	41.33	1.604
10	10 years operational	41.71	1.592

The reported values correspond to the maximum deformation observed in the wall facing or MSE structure.

Analysis Results: Anchor only, without Cross Necklace and Startail

This PLAXIS 3D model considers the Anchor only, without the Cross Necklace or Startail components. The purpose of this configuration is to evaluate the effect of removing both the Cross Necklace and Startail on anchor performance and soil–structure interaction.

The summary of the modelling results for the Anchor, without the Cross Necklace of bars and Startail is presented in Table 22.

Table 22. The summary of analysis results for modelling scenario 11 (compiled by the authors)

No	Construction Stages	Horizontal Facing Deformation (Ux) (mm)	SF
1	Put on MSE, Stack, Put Anchor 1	7.203	6.620
2	Put on MSE, Stack, Put Anchor 2	10.54	3.816
3	Put on MSE, Stack, Put Anchor 3	15.4	2.529
4	Put on MSE, Stack, Put Anchor 4	19.12	2.094
5	Put on MSE, Stack, Put Anchor 5	32.01	1.909
6	Put on MSE, Stack, Put Anchor 6	42.68	1.540
7	Put on MSE, Stack, Put Anchor 7	56.08	1.560
8	Final Construction	66.2	1.481
9	1 year operational	103.38	1.444
10	10 years operational	105	1.442

The reported values correspond to the maximum deformation observed in the wall facing or MSE structure.

Based on the results of the PLAXIS 3D modelling conducted for the 11 configurations, the summary of key outcomes is presented in Table 23.

Table 23. The summary of final analysis results for modeling 11 configurations (compiled by the authors)

No	Modeling Type	The Largest Horizontal Facing Deformation (Ux) (mm)		Smallest FoS	
1	CTC 30 cm + Cross Necklace 15x15 cm	44.58	Safe	1.58	Safe
2	CTC 50 cm + Cross Necklace 15x15 cm	51.27	Safe	1.55	Safe
3	CTC 70 cm + Cross Necklace 15x15 cm	59.72	Safe	1.52	Safe
4	Without *Startail* + CTC 30 cm + Cross Necklace 15x15 cm	68.17	Safe	1.56	Safe
5	Without *Startail* + CTC 30 cm + Cross Necklace 30x30 cm	65.84	Safe	1.53	Safe
6	Without *Startail* + CTC 30 cm + Cross Necklace 40x40 cm	62.26	Safe	1.53	Safe
7	*Startail* + Anchor only	68.09	Safe	1.51	Safe
8	CTC 30 cm + Cross Necklace 30x30 cm	30.50	Safe	1.67	Safe
9	CTC 50 cm + Cross Necklace 30x30 cm	35.25	Safe	1.64	Safe
10	CTC 70 cm + Cross Necklace 30x30 cm	41.71	Safe	1.59	Safe
11	Anchor only	105	Not Safe	1.44	Not Safe

4. Conclusions

4.1. Overall Summary

This study develops and evaluates reinforcement configurations for mechanically stabilized earth (MSE) walls incorporating Cross Necklace and Startail ("Fish Fins") elements in combination with anchors. In all tested configurations, factors of safety (FoS) against overturning, sliding, foundation bearing capacity, and anchor failure exceeded the target value of 1.5, as specified in SNI 8460:2017. Backfill using red soil achieved a dry density corresponding to a California Bearing Ratio (CBR) of 9.5%, surpassing the minimum requirement of 6.5%.

Tensile testing of Cross Necklace anchors revealed higher tensile demand at lower elevations, consistent with increased overburden pressure with depth. Deformation analyses demonstrated that models with center-to-center (CTC) spacings of 30, 50, and 70 cm satisfied both displacement limits and FoS requirements. Effective reinforcement lengths for anchors, Cross Necklaces, and Startails ranged from 0.5 to 0.7 H (where H is wall height), with anchors extending beyond the active failure wedge at the recommended inclination of 45° + φ/2.

Among the configurations evaluated, the 30 × 30 cm Cross Necklace with a CTC spacing of 30 cm yielded the smallest horizontal displacement and the highest FoS, indicating superior performance. Tighter CTC spacing generally enhanced stability and reduced deformation. In contrast, models without a Cross Necklace or with anchors only exhibited significantly greater lateral displacement and lower FoS, with some configurations failing to meet the minimum stability criteria.

4.2. Implications

An MSE wall system incorporating Anchors with Cross Necklace and Startail reinforcement and utilizing red soil as backfill in place of conventional sand–gravel (sirtu) mixtures, can satisfy both technical performance requirements and compliance standards specified in SNI 8460:2017. This approach is applicable to retaining structures for bridge approach embankments, abutments, highways, and railways with grade differentials, as well as other slope stabilization projects. It presents a viable alternative to conventional MSE solutions that rely on geotextile or strip-type reinforcement, particularly in regions where red soil is abundant and granular backfill is scarce or costly.

4.3. Limitations

Field experiments were conducted on a scaled wall segment measuring 1.5 m in height, 1.7 m in width, and 2.5 m in length, to assess horizontal pull-out behavior. In the physical testing, center-to-center (CTC) spacing for the Cross Necklace was limited to 30 cm and 50 cm. The study did not include vertical pull-out tests, nor was it conducted on an in-service bridge site. Broader validation is required to extend the findings to larger CTC spacings (e.g., 70, 100, 150, 200, and 250 cm), evaluate vertical pull-out resistance, and assess performance under representative operational conditions.

4.4. Suggestions for Future Research

Future research should focus on the following key areas:

conducting vertical pull-out tests to complement the existing horizontal pull-out data;

expanding the parametric studies to include a broader range of center-to-center (CTC) spacings and geometric configurations;

performing instrumented, full-scale field trials on bridge approach embankments and transportation corridors to validate laboratory and numerical findings under real-world conditions; and

integrating field monitoring data with 3D finite-element modelling (e.g., PLAXIS 3D) to investigate hydro-mechanical coupling effects, such as rainfall infiltration and elevated pore-water pressures, and assess long-term performance under operational loading.

Declarations

Author Contributions

Conceptualization, K. and R.S.; methodology, K.; software, I.N.H.; validation, K. and R.S.; formal analysis, K.; investigation, K. and R.S.; resources, I.N.H.; data curation, R.S.; writing—original draft preparation, all authors contributed equally; writing—review and editing, K.; visualization, I.N.H.; supervision, R.S.; project administration, K. All authors have read and agreed to the published version of the manuscript.

Data Availability Statement

The data presented in this study are available on request from the corresponding author.

Funding

Funding information is not available.

Conflicts of Interest

The authors declare that there is no conflict of interest regarding the publication of this manuscript.

References

[1] FHWA. *Design and Construction of Mechanically Stabilized Earth (MSE) Walls*. FHWA-HIF-24-002. U.S. Federal Highway Administration, 2023.

[2] EUROCODE 7. Retaining structures: treatment of water levels and design situations (worked examples and guidance). In: *EN 1997-1 Background & Applications—Geotechnical Design with Worked Examples*, 2013.

[3] KOERNER RM, & KOERNER GR. A data base, statistics and recommendations regarding 171 failed geosynthetic reinforced mechanically stabilized earth (MSE) walls. *Geotextiles and Geomembranes*, 2013, 40: 20–27. https://doi.org/10.1016/j.geotexmem.2013.06.001

[4] KOERNER RM, & KOERNER GR. An extended data base and recommendations regarding 320 failed geosynthetic reinforced mechanically stabilized earth (MSE) walls. *Geotextiles and Geomembranes*, 2018, 46(6): 904–912. https://doi.org/10.1016/j.geotexmem.2018.07.013

[5] KOERNER RM, & KOERNER GR. The importance of drainage control for geosynthetic-reinforced MSE walls. *Journal of GeoEngineering*, 2011, 6(1): 1–12. http://doi.org/10.6310/jog.2011.6(1).1

[6] YANG K-H, WU H-M, TSENG T-L, & YOO C. Model tests of geosynthetic-reinforced soil walls with marginal backfill subjected to rainfall. *Geotextiles and Geomembranes*, 2023, 51(2): 342–359. https://doi.org/10.1016/j.geotexmem.2022.12.002

[7] FHWA. *MSE Walls and RSS—Design and Construction Guidelines*. FHWA-NHI-10-024. U.S. Federal Highway Administration, 2009.
[8] JAYANANDAN M, & VISWANADHAM BVS. DIA/centrifuge studies on geogrid or hybrid geosynthetic-reinforced soil walls under rainfall infiltration. *Geotextiles and Geomembranes*, 2023, 51(4): 36-55. https://doi.org/10.1016/j.geotexmem.2023.03.002
[9] BADAN STANDARDISASI NASIONAL (BSN). *SNI 8460:2017—Persyaratan Perancangan Geoteknik*. Jakarta: BSN; 2017. (see official PDF hosted by Ditjen Bina Marga). binamarga.pu.go.id
[10] Federal Highway Administration (FHWA). *Design and Construction of Mechanically Stabilized Earth Walls and Reinforced Soil Slopes (MSE/RSS)*. FHWA-NHI-10-024; 2009.
[11] ASTM International. *ASTM D6706—Standard Test Method for Measuring Geosynthetic Pullout Resistance in Soil*; reapproved 2021.
[12] TRANSPORTATION RESEARCH BOARD (TRB). *Use of Inclinometers for Geotechnical Instrumentation on Transportation Projects*. TRB Circular EC129, 2008.
[13] ANDERSON, D.G, MARTIN, G.R., LAM, I.P. & WANG, J.N. Seismic Analysis and Design of Retaining Walls, Buried Structures, Slopes, and Embankments, NCHRP Report 611, USA, 2008. https://www.ce.memphis.edu/7137/PDFs/Seismic%20Manual/nchrp_rpt_611.pdf
[14] BATHURST, R., SIMAC, M., & BERG, R. Review of NCMA Segmental Retaining Wall Design Manual for Geosynthetic-Reinforced Structures. Transportation Research Record, No. 1414: 16–25. Washington, DC, 1993. https://onlinepubs.trb.org/Onlinepubs/trr/1993/1414/1414-004.pdf
[15] CHRISTOPER BR, ELIAS V, & BERG RR. Mechanically Stabilized Earth Walls and Reinforced Soil Slopes. Design and Construction Guidelines. FHWA-NHI-00-043. National Highway Institute Federal Highway Administration US Department of Transportation. Washington DC, 2001. https://vulcanhammer.net/wp-content/uploads/2017/01/fhwa-nhi-00-043.pdf
[16] DAS B. M. *Principles of Geotechnical Engineering*, Sixth Edition, Boston, Pws-Kent Publishing Company, 2010.
[17] OVESEN N. K., and STRØMANN H. Design Method for Vertical Anchor Slabs in Sand. *Proceedings of Specialty Conference on Performance of Earth and Earth-Supported Structures*, 1973, 1–2: 1418–1500. https://cedb.asce.org/CEDBsearch/record.jsp?dockey=0265141
[18] STANDARDS AUSTRALIA. Earth-retaining structures. Designation: AS 4678-2002 AMDT 1. SDO: SA, 2003.
[19] DAS B. M. *Principles of Foundation Engineering*, Seventh Edition, Boston, Pws-Kent Publishing Company, 2011.
[20] AMERATUNGA J., SIVAKUGAN N., & DAS B.M. Correlations of Soil and Rock Properties in Geotechnical Engineering. Springer, New Delhi, 2016. https://doi.org/10.1007/978-81-322-2629-1
[21] LOOK B.G. *Handbook of Geotechnical Investigation and Design Tables*: Second Edition (2nd ed.). CRC Press, 2014. https://doi.org/10.1201/b16520
[22] DHAMDHERE DR, RATHI VR, & KOLASE PK. Design and Analysis of Retaining Wall. *International Journal of Technology and Engineering*, 2018, 8(9): 1246-1263. https://www.researchgate.net/publication/358459814_DESIGN_AND_ANALYSIS_OF_RETAINING_WALL

参考文:

[1] 美国联邦公路管理局 (FHWA)。机械稳定土 (MSE) 墙的设计与施工。FHWA-HIF-24-002。
美国联邦公路管理局，2023 。
[2] 欧洲规范 7。 挡土结构： 水位处理和设计情况（实例和指导）。见：EN 1997-1 背景与应用——岩土工程设计与实例，2013。
[3] KOERNER RM 和 KOERNER GR。关于 171 处失效土工合成材料加筋机械稳定土 (MSE) 墙的数据库、 统计数据和建议。 土工布和土工膜，2013，40: 20-27。https://doi.org/10.1016/j.geotexmem.2013.06.001
[4] KOERNER RM 和 KOERNER GR。关于320个失效土工合成材料加筋机械稳定土（MSE）墙的扩展数据库和建议。《土工布和土工膜》.2018，46(6): 904–912。https://doi.org/10.1016/j.geotexmem.2018.07.013
[5] KOERNER RM 和 KOERNER GR。排水控制对土工合成材料加筋机械稳定土墙的重要性。 《土工工程学报》.2011.6(1): 1–12。http://doi.org/10.6310/jog.2011.6(1).1
[6] YANG K-H, WU H-M, TSENG T-L 和 YOO C. 带边缘回填土的土工合成材料加筋土墙降雨模型试验。土工布和土工膜，2023，51(2): 342–359。https://doi.org/10.1016/j.geotexmem.2022.12.002
[7] 美国联邦公路管理局 (FHWA)。MSE 墙体和 RSS——设计和施工指南。FHWA-NHI-10-024。
美国联邦公路管理局，2009。
[8] JAYANANDAN M 和 VISWANADHAM BVS。降雨入渗条件下土工格栅或混合土工合成材料加筋土墙的 DIA/离心机研究。 土工布和土工膜，2023，51(4): 36-55。https://doi.org/10.1016/j.geotexmem.2023.03.002
[9] 国家标准局 (BSN)。SNI 8460:2017——土工技术试验。雅加达：BSN；2017。（参见 Ditjen Bina Marga 托管的官方 PDF）。binamarga.pu.go.id
[10] 联邦公路管理局 (FHWA)。机械稳定土墙和加筋土坡的设计和施工 (MSE/RSS)。FHWA-NHI-10-024；2009。
[11] 美国材料与试验协会 (ASTM) 标准。ASTM

D6706——测量土工合成材料在土壤中的抗拔力的标准试验方法；2021年重新批准。

[12] 交通研究委员会 (TRB)。倾角仪在交通项目中作为岩土仪器的使用。 TRB 通函 EC129.2008。

[13] ANDERSON, D.G.、MARTIN, G.R.、LAM, I.P. 和 WANG, J.N. 挡土墙、地下结构、斜坡和路堤的抗震分析与设计， NCHRP 报告 611，美国.2008。https://www.ce.memphis.edu/7137/PDFs/Seismic%20Manual/nchrp_rpt_611.pdf

[14] BATHURST, R.、SIMAC, M. 和 BERG, R.《NCMA土工合成材料加筋结构分段式挡土墙设计手册》综述。《交通研究记录》，第1414号：16-25页。华盛顿特区.1993。https://onlinepubs.trb.org/Onlinepubs/trr/1993/1414/1414-004.pdf

[15] CHRISTOPER BR、ELIAS V、BERG RR。《机械稳定土墙与加筋土坡》。设计与施工指南。FHWA-NHI-00-043。 美国国家公路研究所，美国联邦公路管理局， 美国交通部。 华盛顿特区，2001。 https://vulcanhammer.net/wp-content/uploads/2017/01/fhwa-nhi-00-043.pdf

[16] DAS B. M. 《岩土工程原理》，第六版，波士顿，Pws-Kent Publishing Company，2010。

[17] OVESEN N. K. 和 STRØMANN H.《砂土中垂直锚板的设计方法》。 《土体及土体支撑结构性能专业会议论文集》， 1973， 1-2：1418-1500。https://cedb.asce.org/CEDBsearch/record.jsp?dockey=0265141

[18] 澳大利亚标准协会。 《挡土结构》。 名称：AS 4678-2002 AMDT 1。 SDO：SA.2003。

[19] DAS B. M. 《基础工程原理》， 第七版， 波士顿， Pws-Kent 出版公司.2011。

[20] AMERATUNGA J.、SIVAKUGAN N. 和 DAS B.M.《岩土工程中土与岩石特性的相关性》。Springer，新德里.2016。https://doi.org/10.1007/978-81-322-2629-1

[21] LOOK B.G.《岩土工程勘察与设计表手册》第二版。 CRC Press，2014。https://doi.org/10.1201/b16520

[22] DHAMDHERE DR、RATHI VR 和 KOLASE PK。挡土墙设计与分析。《国际技术与工程杂志》.2018，8(9): 1246-1263。https://www.researchgate.net/publication/358459814_DESIGN_AND_ANALYSIS_OF_RETAINING_WALL

Word count (excluding references): 12,142 words.

Peer-review record:
- ***Fast-track status:*** Not fast-tracked
- ***First-round reviews received:*** 3 reports
- ***Revision cycles completed:*** 3 rounds
- ***Final version submitted:*** July 9, 2025

Disclaimer/Publisher’s Note:

Appendix A

A. Soil Retaining Wall Data

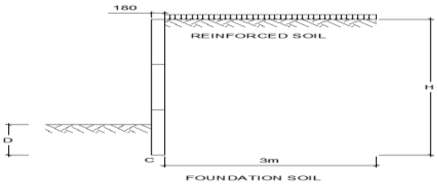

1. Soil data

H	=	4.50	m
$\gamma 1$	=	19.0	kN/m3
Φ1	=	30.00	°
c'1	=	15.00	kN/m2
$\gamma 2$	=	20.00	kN/m3
Φ2	=	28.00	°
c'2	=	30.00	kN/m2
Q	=	15.00	kN/m2
γc (concrete)	=	24.00	kN/m3
γl (soil)	=	27.00	kN/m3
D	=	1.00	m
α	=	0.00	°

2. Data PC segmental retaining wall

Width (B)	=	1.50	m
Height (H)	=	1.50	m
Thickness (T)	=	0.18	m
Area	=	2.31	m2
Weight	=	997.14	kg /pcs
Quality of Concrete	=	K-500	
fc'	=	41.50	MPa

Calculation of Lateral Soil Pressure

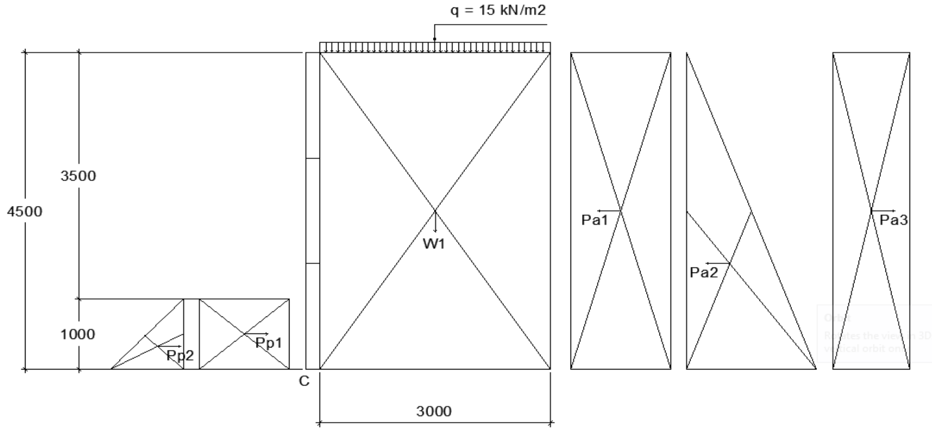

Vertical style:

W1	=	L x γ1 x H	
	=	256.5	kN/m
Weight of 1 panel	=	997.14	
	=	9.97	
Weight of 3 panels	=	29.91	
Wall weight/m'	=	Weight of 3 panels/Panel width	
	=	19.9428	kN/m

Active soil pressure			
A	=	0.00	°
Θ	=	0.00	°
Φ1	=	30.00	°
because Φ1, then Ka	=	0.33	
Consequences of the load working on the wall			
Pa1	=	Ka x H x q	
	=	22.275	
Consequences of the load of the soil layer of the heap			
Pa2	=	1/2 x Ka x H^2 x Y1	
	=	63.48375	kN/m
Pa3	=	-2C2 √(Ka x H)	
	=	-36.558173	kN/m
Passive ground pressure		$\tan^2(45 + \frac{\Phi'_2}{2})$	
Kp	=		
	=	2.77	kN/m
Pp1	=	$\frac{1}{2}\ x\ Kp\ x\ D^2 x\ \gamma_2$	
	=	27.70	kN/m
Pp2	=	$2c_2\sqrt{Kp\ x\ D}$	
	=	99.86	kN/m

Vertical Moment Against Point C

No	Style (kN/m)		Distance to point C (m)
	(1)		(2)
1.00	W1 =	256.50	1.68
2.00	W2 =	19.94	0,09
	∑ Pv =	**276.44**	

Active Moment Against Point C

No	Style (kN/m)		Distance to point C (m)
	(1)		(2)
1.00	Pa1 =	22.28	2.25
2.00	Pa2 =	63.48	1.50
3.00	Pa3 =	-36.56	2.25
	∑ Pa =	**49.20**	

Passive Moment toward point C

No	Style (kN/m)		Distance to point C (m)
	(1)		(2)
1.00	Pp1 =	27.70	0.50
2.00	Pp2 =	99.86	0.33
	∑ Pp =	**127.56**	

Stability Analysis Against *Overturning*			
The moment that resulted in the overthrow			
∑ Mg	=	∑ Ma	
	=	63,09	
The moment that resisted the overthrow			
∑ Mw	=	∑ Mv + ∑ Mp	
	=	479.84	
SF roll (overturning)			
SF roll	=	∑ Mw / ∑ Mg	
SF roll	**=**	**7.60564273**	>
Slider Stability Analysis			
SF Geser	=	F / ∑ Pa	
∑ Pa	=	49.20	kN/m
Forces that counteract shear forces F	=	$\left\{cg + \left(\frac{W}{l_g}\right)\text{tg}\,\delta\right\} l_g$	
Cg	=	β x C2	
	=	20.00	kN/m2
Ig	=	3	m
W	=	Lebar x H x Y1	
	=	256.5	kN/m
$\text{tg}\,\delta$	=	$\beta\ x\,\text{tg}\,28$	
	=	0.35	
F	=	$\left\{cg + \left(\frac{W}{l_g}\right)\text{tg}\,\delta\right\} l_g$	
	=	150.92	kN/m
SF Slide	=	F / ∑ Pa	
SF Slide	**=**	**3,0674907**	>
σ_{ult}	=		
Φ2	=	28.00	
c'2	=	30	kN/m2
γ2	=	20.00	kN/m3

φ	N_c	N_q	$N_{\gamma(H)}$	$N_{\gamma(M)}$	$N_{\gamma(V)}$	N_q/N_c	2tanφ(1-sinφ)^2
0	5,14	1,0	0,0	0,0	0,0	0,195	0,000
5	6,49	1,6	0,1	0,1	0,4	0,242	0,146
10	8,34	2,5	0,4	0,4	1,2	0,296	0,241
15	10,97	3,9	1,2	1,1	2,6	0,359	0,294
20	14,83	6,4	2,9	2,9	5,4	0,431	0,315
25	20,71	10,7	6,8	6,8	10,9	0,514	0,311
26	22,25	11,8	7,9	8,0	12,5	0,533	0,308
28	25,79	14,7	10,9	11,2	16,7	0,570	0,299
30	30,13	18,4	15,1	15,7	22,4	0,610	0,289
32	35,47	23,2	20,8	22,0	30,2	0,653	0,276
34	42,14	29,4	28,7	31,1	41,0	0,698	0,262
36	50,55	37,7	40,0	44,4	56,2	0,746	0,247
38	61,31	48,9	56,1	64,0	77,9	0,797	0,231
40	75,25	64,1	79,4	93,6	109,3	0,852	0,214
45	133,73	134,7	200,5	262,3	271,3	1,007	0,172
50	266,50	318,5	567,4	871,7	761,3	1,195	0,131

m

From the table, we get:

Nc	=	25.79	
Nq	=	14.70	
Ny	=	10.90	
σ_{ult} Therefore,	=		
$\sigma_{terjadi}$	=	1100.70	kN/m2
	=	$H\,x\,\gamma_2 + q$	
	=	105.00	kN/m2
SF Bearing	=	$\frac{\sigma_{ult}}{\sigma_{terjadi}}$	
	=	**10.4828571**	>

Anchor data

fy'	=	280.00	MPa
D Anchor	=	19.00	mm
Quantity per panel	=	4.00	bh

Anchor Length Analysis

Height of each precast			
Precast 1	=	1.50	m
Precast 2	=	1.50	m
Precast 3	=	1.50	m
Tinggi Z1 (Emphasis point between precasts)			
Precast 1	=	3.75	m
Precast 2	=	2.25	m
Precast 3	=	0.75	m
Anchor position on the precast from the Z1 position (x)			
Precast 1	=	0.50	m
Precast 2	=	0.50	m
Precast 3	=	0.50	m

		Anchor 1	
Z	=	Z1 ± x	
Therefore, z			
Precast 1	=	4.25	m
Precast 2	=	2.75	m
Precast 3	=	1.25	m

Anchor length

L = $$\frac{H - z_i}{\tan(45 + \frac{\phi}{2})}$$

ϕ

	=	19.00	mm
	=	0.019	m

Therefore,

Precast	Anchor	zi (m)	L (m)
1	1	4.25	0.25
	2	3.25	1.25
2	1	2.75	1.75
	2	1.75	2.75
3	1	1.25	3.25
	2	0.25	4.25

Safety Factor Analysis

Q	=	15.00	
$\gamma 1$	=	19.00	kN/m3
Ka	=	0.33	
A Anchor	=	$\pi D \ x \ L_i$	
σ_h	=	$Ka \ x \ q + Ka \ x \ \gamma_1 \ x \ zi$	
Δ_{ph}	=	$\sigma_h \ x \ Sh \ x \ Sv$	
Sh	=	1	m
Sv	=	1	m
fy'	=	280.00	Mpa
σ_{ijin}	=	fy' x A Anchor	
SF Pull Anchor	=	$\frac{\sigma \ ijin}{\Delta_{ph}}$	

Therefore:

	(1)	(2)	(3)
Precast	Anchor	zi (m)	Li (m)
1	1	4.25	5.00
	2	3.25	5.00
2	1	2.75	5.00
	2	1.75	5.00
3	1	1.25	5.00
	2	0.25	5.00

(6)
Δ_{ph}
31.6
25.33
22.19
15.92
12.79
6.52